Conf-751130--8

PREPRINT UCRL- 77041

Lawrence Livermore Laboratory

MODELS OF ELECTRON CONDUCTIVITY WHICH LEAD TO ABLATION STABILIZATION OF FLUID INSTABILITIES IN LASER-DRIVEN IMPLOSIONS

J. D. Lindl and W. C. Mead

October 17, 1975

This paper was prepared for presentation at the American Physical Society Meeting, Plasma Physics Div., St. Petersburg, Florida November 10-14, 1975

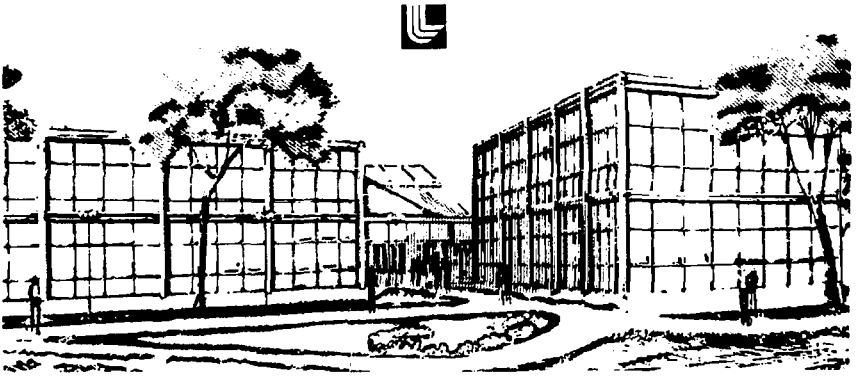

Models of Electron Conductivity Which Lead to Ablation Stabilization of Fluid Instabilities in Laser-Driven Implosions*

J. D. Lindl and W. C. Mead

University of California, Lawrence Livermore Laboratory
Livermore, California 94550

Ablation Stabilization

Introduction

In previous work,[1] the authors have conducted a systematic study of fluid instabilities arising during the implosion of a low entropy DT shell. The use of shell-type targets is of great interest because of the lower power requirements imposed relative to a solid sphere target of the same mass. Fluid instability puts a limit on the aspect ratio r/Δr that one can use where r is the target radius and Δr the shell thickness. The limitation arises because the fluid instability can result in mixing of high and low density and high and low temperature matter, thus greatly reducing the compression one could achieve. The conclusions of our previous work are two-fold.

*Research performed under the auspices of the U. S. Energy, Research and Development Administration. Contract No. W7405-ENG-48

1. The fluid instabilities grow at rates close to the classical value $\exp(\gamma t)$ where $\gamma = \sqrt{ka}$ (k is the wavenumber and a is the acceleration).
2. To survive such instabilities, one has to use low aspect ratio shells with $r/\Delta r \sim 2\text{-}3$ and use impulsive acceleration by driving the shell with a series of shock waves.

Theoretical work by Bodner[2] and Leith[3] predicts the existence of an ablation stabilizing mechanism under various assumptions about the zero order solution and thermal conduction.

In order to obtain confidence in the above conclusions for isentropic implosions, and an understanding of why the fluid instabilities were not stabilized, it is of considerable interest to try to reproduce the conditions assumed by the model calculations of Bodner and Leith. If that is done, it is possible to understand just what features of the physics are responsible for stabilization and understand what is not satisfied in the isentropic implosions.

Firepolishing as a Stabilization Mechanism

The most prominent feature of the zero-order solution assumed by both Bodner and Leith is the existence of a sharply defined ablation front across which there exists a discontinuity in pressure, temperature and density. The pressure drop across

the ablation surface is the ablation pressure. It is not a thermal pressure, but an inertial reaction pressure generated when material ablates. Hence, at the ablation front, there is a discontinuity in the thermal pressure. This feature is missing in electron-driven implosions. Figure 1 is a plot of pressure, temperature and density as a function of position for a typical isentropically imploded DT shell. The density drops rapidly as it is ablated. But the pressure in the vicinity of the ablation surface is slowly varying. This feature is determined by the electron conductivity. If F is the flux of energy transported by the electrons, then $F \alpha \rho \lambda v_{th} \nabla T$ which is essentially independent of ρ since λ is inversely proportional to density. For a given flux and temperature, ∇T depends only on the grams per square centimeter needed to stop an electron. As the electrons run up the density gradient at the ablation surface, the number of grams per square centimeter they go through per unit distance increases so ∇T must increase in order for the electrons to carry the flux required to drive the ablation. To keep the flux about constant, $\nabla T/T$ is about equal to $\nabla \rho/\rho$ so that $\rho T \sim$ const resulting in the flat pressure profile seen in Figure 1. This means that for the typical electron ablation-driven implosion, there is no true ablation pressure as defined above. If the above explanation is correct, then one ought to be able to produce an implosion with a sharp pressure drop at

the ablation surface by artificially modifying the thermal conductivity so the flux depends strongly on the density. Such a modification would result in electron energy deposition in a thin layer near the ablation surface. In the computer code, LASNEX[4], written by George Zimmerman of LLL, we have done this by introducing a coefficient of thermal conductivity K such that $K\alpha T^n/\rho^m$ where n and m can be varied. Such a dependence has been used in the implosion of various targets. A typical example is shown in Figure 2A. A perturbation is applied to the shell in Region 1 and energy is introduced into the low density Region 2. For the temperature profile shown in Figure 2B using n = 6.5 and m = 3, pressure profiles such as that in Figure 3 result. A clear ablation front is visible with more than half the pressure being generated by the ablation process at the surface. Also shown in Figure 3 are the density and temperature profiles. It is not possible to keep each of these quantities constant on either side of the ablation surface as postulated in the theoretical work, but they are slowly varying.

The Leith theory of stabilization results in a dispersion relation of the following form

$$\gamma^2 = ka - k^2 P_A/\rho^+ \qquad (1)$$

where k is the wavenumber, a, the acceleration, P_A the ablation

pressure and ρ^+ the shell density. P_A can be calculated from the following model. For a rocket, the rocket velocity is given by

$$v = v_o \ln M_o/m .$$

The rocket acceleration, or ablation acceleration a_A due to blowing off mass is given by

$$a_A = v_o \dot{m}/m.$$

For the case at hand, this acceleration can be considered as due to the ablation pressure so that

$$a_A \dot{m}/m = a_A \Delta\dot{x}/\Delta x = P_A / \rho^+ \Delta x \quad \text{or}$$

$$P_A = \rho^+ v_o \Delta\dot{x}$$

where Δx is the shell thickness and $\Delta\dot{x}$ is the velocity of the ablation front through the shell.

By conservation of mass

$$\rho^+ \Delta\dot{x} = \rho^- v_o$$

where ρ^- is the density in the blowoff or $P_A = \rho^- v_o^2$. This expression does give the correct value for the pressure jump such as seen in Figure 2. Substituting this in Equation 1 gives the shortest unstable wavelength as

$$\lambda_{CL} = 2\pi/K_{CL} = 2\pi\rho^-/\rho^+\left(v_o^2/a\right) = 2\pi P_A/\rho^+ a$$

The dispersion relation becomes

$$\gamma^2 = Ka(1 - K/K_{CL}) \qquad (2)$$

The fastest growing mode is for $K = K_{CL}/2$.

Bodner's theory includes convective terms not in Leith's theory. These terms add considerably to the complexity of the dispersion relation which becomes a cubic equation. In the limit of $\varepsilon = \rho^-/\rho^+ \to 0$, Bodner's dispersion relation gives

$$K_{CB} = \frac{a\rho^+}{\beta^+ P^+} \quad \text{where} \quad \beta = 1 + \frac{(P^+)dv_o/dt}{v_o d(P^+)/dt}$$

K_{CB} is the maximum K for instability. If you interpret β as the fraction of the total pressure which is due to ablation, then $K_{CB} = K_{CL}$. In fact, for the cases we have analyzed, K_{CB} is about equal to K_{CL}. Also if one takes the limit of Bodner's

dispersion relation for the case when $U^2 = Kv_o^2/g >> 1$ which is true here and ignore $\epsilon = \rho^-/\rho^+$ terms, one obtains the dispersion relation

$$\gamma^2 = Ka\ (1 - K/K_{CE}) \tag{3}$$

which is the same as Equation 2.

Finite ϵ effects act to decrease the worst unstable wavenumber K_{max} and changes the dispersion relation such that $\gamma / \sqrt{Ka}$ becomes approximately linearly with $(1 - k/K_{max})$ for cases studied here.

To look at the growth of perturbations, we have applied a ZIG-ZAG deformation to a spherical shell. We have zoned these perturbations using 4 azimuthal zones per wavelength. The calculations look at a conical section of a sphere. The cone half-angle is chosen to be an integral number of half wavelengths of the spherical harmonic under investigation.

A detailed examination of the justification of this method can be found in References 1 and 5. Use of 4 zones per wavelength allows us to isolate a single mode at a time. The principal systematic error introduced by use of 4 zones per wavelength is 15-20% damping of the growth for classical fluid instability test problems.

The measured dispersion relation for the target in Figure 2 is shown in Figure 4. These values are averages between times

2.2 ns and 3.39 ns. The amplitude versus time is plotted in Figure 5 for several spherical harmonics. Also plotted in Figure 4 are the $\epsilon = 0$ and finite ϵ versions of Bodner's dispersion relation for the calculational conditions. The range of theoretical values arises from the fact that the various parameters involved change during the calculation. The rapid dropoff in $\gamma/\gamma_{classical}$ for the smaller K values is qualitatively consistent with the theoretical model. However, the calculated values tend to level out at large K instead of dropping to zero. This may be due to a breakdown of one of the assumptions in Bodner's model. He assumed KL = 1 in arriving at his dispersion relation. L is the scale height for decay of thermal perturbations generated at the ablation surface. This is satisfied quite well for the longer wavelengths but starts to break down for the shorter wavelengths. The RMS variation in Te as a function of position at time = 3.39 ns is shown in Figure 6 for $\ell = 50$ and $\ell = 600$. KL versus K is shown in Figure 7. That KL > 1 should lead to a decrease in the stabilizing effect is reasonable. Figure 8 shows a model of the firepolishing effect we are considering here. Because the peaks of the perturbation are closer to the constant temperature surface, the temperature gradient there is larger which induces a higher ablation rate which drives the peak back. If the constant temperature surface is further from the perturbed surface, the firepolishing effect gets weaker.

This is the effect of having KL > 1. It means one has to go further from the perturbed surface to reach a given degree of uniformity in the temperature.

Convection and Finite Density Gradient Stabilization

In the case of $\beta = 0$, Bodner's dispersion relation for KL = 1 becomes

$$\gamma = \sqrt{Ka + 1/4\ K^2V_A^2} - 1/2\ KV_A \qquad (4)$$

For KV_A large, this dispersion relation predicts a decrease in the growth rate just because of convection of material through the ablation surface. The Rayleigh-Taylor instability is a surface phenomenon with amplitudes that decay exponentially as $\exp[K(x-x_o]$ as one moves away from the surface. The rate at which a given amplitude propagates into the material is given by $V \sim \gamma/K$. If the ablation velocity V_A is comparable to this rate, one chews through the material faster than the perturbation can propagate and one would expect stabilization. The criterion for a significant effect becomes $V_A \gtrsim \gamma_{classical}/K$ or $K^2V_A^2 \gtrsim Ka$. Equation 4 gives the result that the growth rate asymptotically approaches a constant value given by $\gamma_{max} = a/V_A$.

The case with $\beta = 0$ is essentially the case when there is no ablation pressure. This is the usual electron-driven implo-

sion condition. Unfortunately, for typical isentropic implosions, V_A is one to two orders of magnitude too low to give a significant effect.

Attempts to model the convective effect have generally been ambiguous. The reason is that when the power is increased sufficiently to generate the high ablation rates needed, the density gradient that results gives a stabilizing behavior very similar to that predicted for the convection. For $\frac{1}{\rho}\frac{d\rho}{dx} = \delta$ Lelevier[6] gets the result that $\gamma^2 = [K\delta/(K + \delta)]a\alpha$ where α is the Atwood number. An example is shown in Figure 9. For this dispersion relation, a "stiff" slab 1μmm thick was accelerated by a 1/4 μ laser delivering 10^{16} Watts per square centimeter. This power generated a pressure of about 500 Megabars. By modifying the equation of state to represent a stiff gas, the slab was kept approximately incompressible. As seen in Figure 9 the LASNEX calculated dispersion relation, the finite density gradient dispersion relation and the convective stabilized dispersion relation are all qualitatively similar. Since the LASNEX values lie uniformly below both the finite density gradient and convective curves, it might be that both effects are contributing. On the other hand, LASNEX has systematic effects which could lower the growth by the observed amount. For now, Equation 4 must be considered untested.

Conclusions

LASNEX calculations with a modified electron conductivity show the existence of a firepolishing stabilization effect. By modifying the thermal conductivity so that $K \alpha T^n/\rho^m$, one is able to construct a situation in which the electrons deposit their energy in a thin layer at the ablation surface and closely match the zero order solutions assumed by Bodner and Leith. The firepolishing effect appears to require that a significant fraction of the total pressure be due to the ablation process itself rather than the thermal pressure in the corona gas. It also requires $KL \sim 1$ where L is the scale height for decay of thermal perturbations generated at the ablation surface. For classical electron conductivity, because the thermal flux depends linearly on the grams/cm^2 necessary to stop the electrons, $(1/\rho)\nabla\rho\sim(1/T)\nabla T$ near the ablation surface so that the pressure is nearly constant across the ablation surface. Hence there is no ablation pressure as such and no firepolishing effect for electron-driven implosions.

In the absence of an ablation pressure, one can convectively stabilize fluid instability or stabilize because of finite density gradients which result from high ablation rates. For implosions of interest in achieving high compression, low entropy configuration, these latter effects are small for the worst unstable wavelengths because the ablation rates are low by an order of magnitude or more.

REFERENCES

1. J. D. Lindl and W. C. Mead, Phys. Rev. Letters, Vol. 34, No. 20 pp 1273-1276.
2. S. E. Bodner, Phys. Rev. Letters, Vol. 33, 761 (1974)
3. C. Leith, private communication.
4. G. B. Zimmerman, LLL Report, UCRL-74811 (unpublished).
5. W. C. Mead and J. D. Lindl, LLL Report UCRL 77057 (unpublished).
6. R. Lelevier, G. Lasher and F. Bjorkland, UCRL 4459, 2-21-55 (unpublished).

PRESSURE, DENSITY AND TEMPERATURE VERSUS RADIUS FOR A D-t SHELL IMPLODED USING SPITZER ELECTRON CONDUCTIVITY

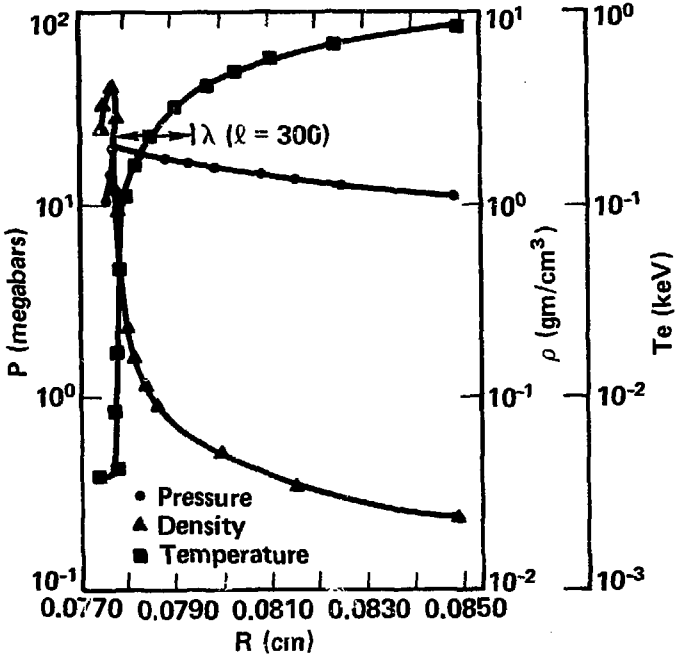

Figure 1

TARGET AND ELECTRON TEMPERATURE USED IN FIREPOLISHING STUDY

Figure 2 (a)

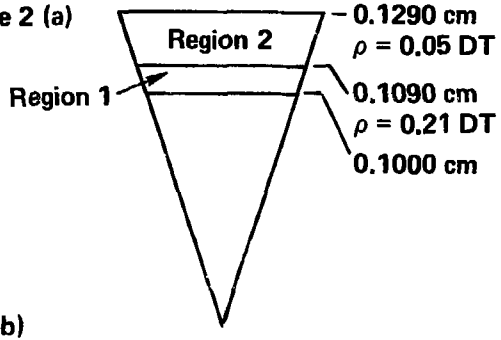

Figure 2 (b)

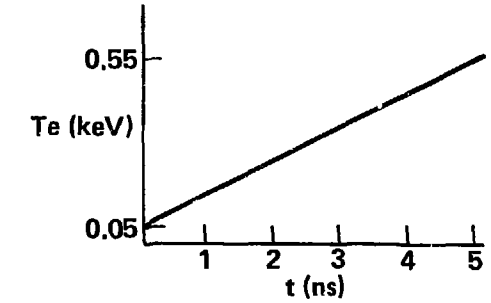

Figure 2

PRESSURE, DENSITY AND TEMPERATURE VERSUS DENSITY FOR FIREPOLISING STABILIZED IMPLOSION

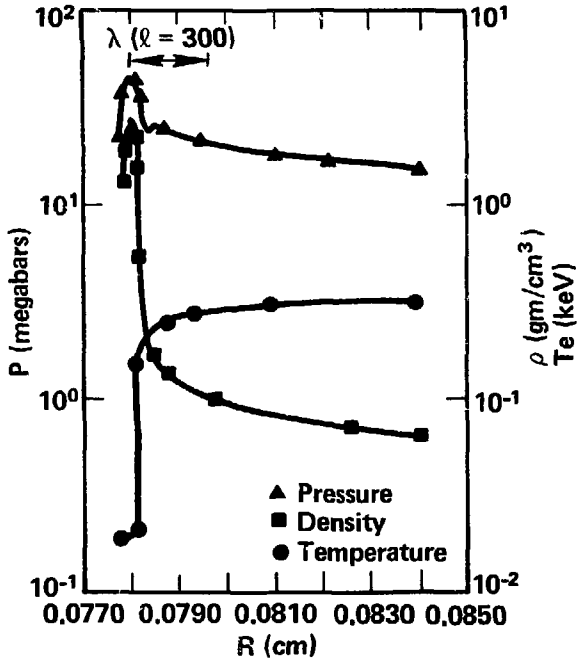

Figure 3

GROWTH RATE VERSUS WAVENUMBER IN FIREPOLISHING REGIME

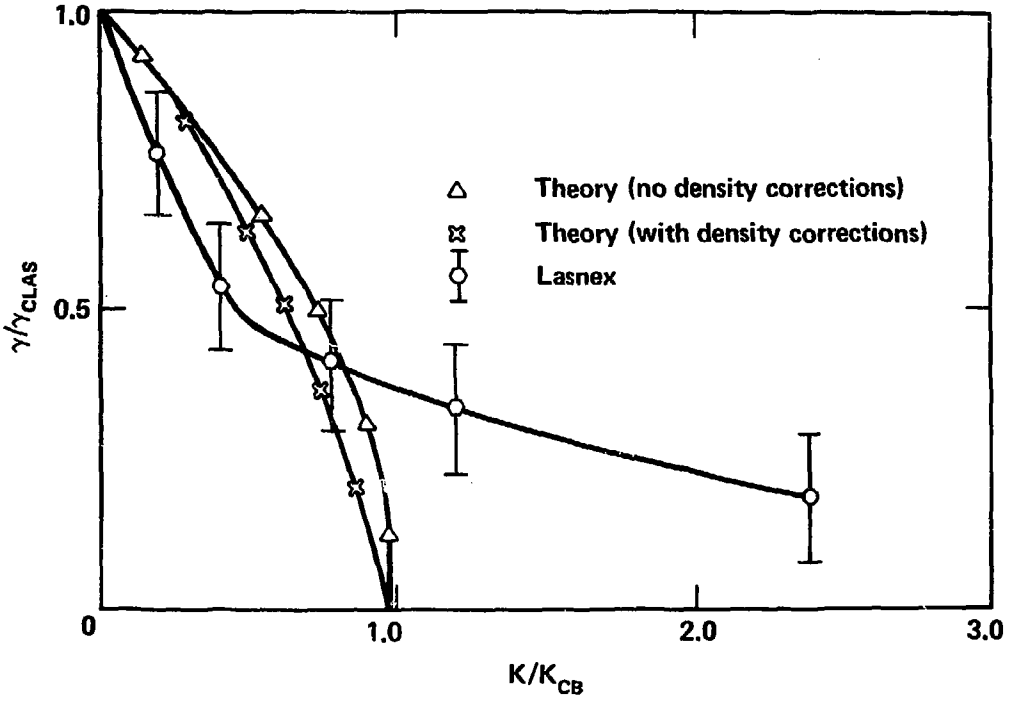

Figure 4

PERTURBATION AMPLITUDE VERSUS TIME IN THE FIREPOLISHING REGIME

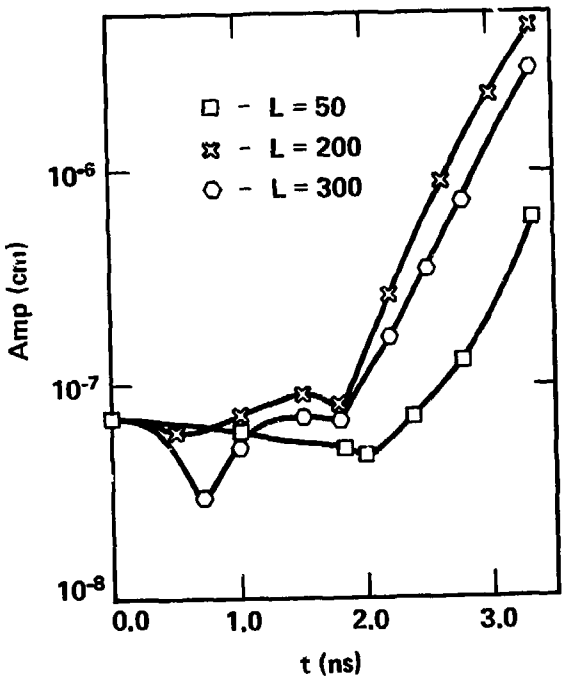

Figure 5

RMS DEVIATION OF ELECTRON TEMPERATURE VERSUS RADIUS

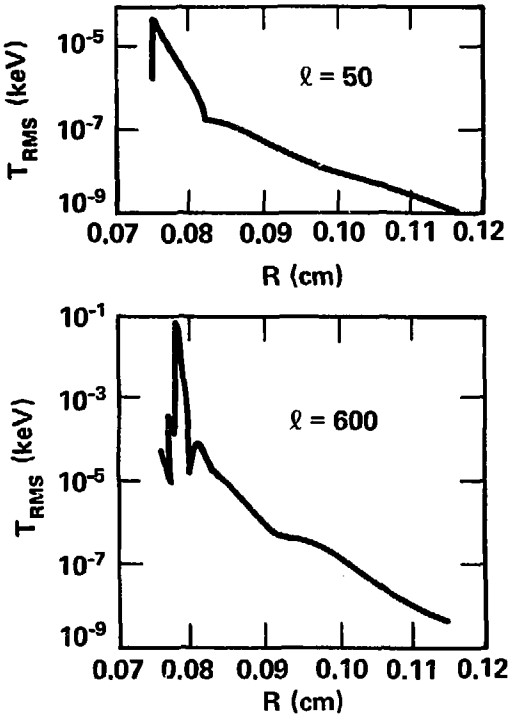

Figure 6

KL VERSUS K/K_{CB} FOR ELECTRON TEMPERATURE PERTURBATIONS

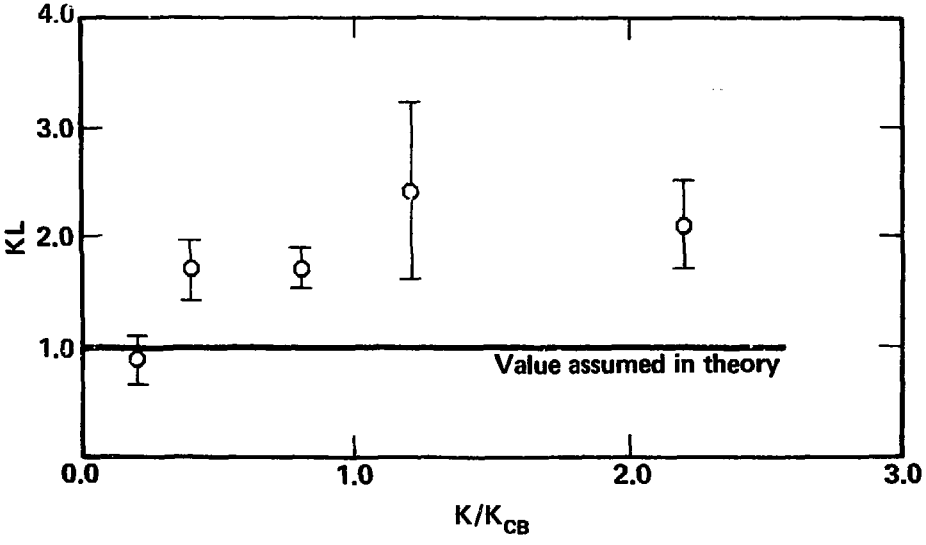

Figure 7

FIREPOLISHING MODEL

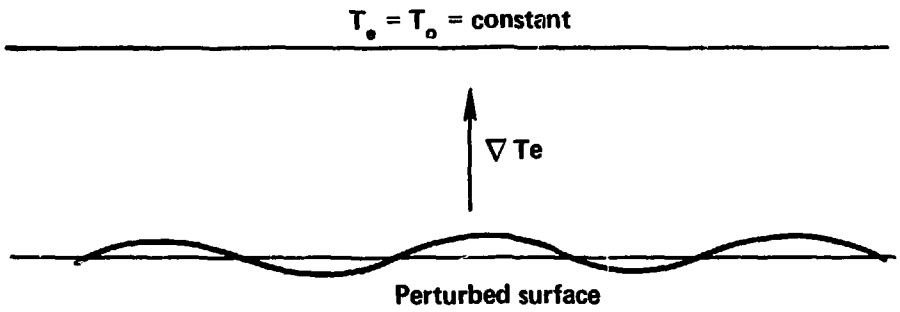

Figure 8

GROWTH RATE VERSUS WAVENUMBER IN THE PRESENCE OF A FINITE DENSITY GRADIENT AND RAPID ABLATION

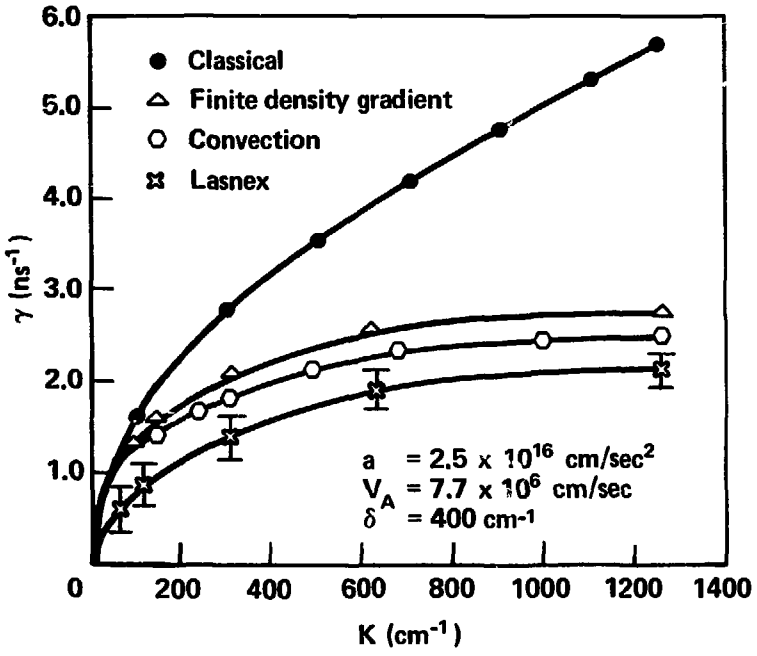

Figure 9